GPS MONITORING NETWORKS:
INTERVAL-BASED DESCRIPTION OF MEASUREMENT
UNCERTAINTIES DUE TO REMAINING SYSTEMATICS

Steffen Schön.[1]
Engineering Geodesy and Measurement Systems
Graz University of Technology, Austria
Email: steffen.schoen@tugraz.at

Hansjörg Kutterer
Geodetic Institute
University of Hannover, Germany
Email: kutterer@gih.uni-hannover.de

Abstract: GPS is an attractive technique for applications in engineering geodesy such as the monitoring of large structures' deformations or of landslides. In order to correctly assess the representativity of the derived motion and deformation terms, the effective uncertainty budget (due to random variability and remaining systematics) has to be modelled adequately. In this study, deterministic error bands (intervals) are used to describe the amount of the remaining systematics in the GPS data. They consist of upper and lower bounds for the observed values which are obtained using a forward modelling approach. The resulting observation intervals quantify the impact of the uncertainty about standard correction models. Their magnitudes depend on the whole satellite-receiver geometry. Finally these intervals are linearly transferred to the estimated point coordinates.

In the paper, two main outcomes are presented and discussed for local monitoring networks (baseline lengths smaller than 5 km). First, for 24h sessions and horizontal networks the maximum uncertainty occurs in baseline direction. Most of this uncertainty is significantly mitigated using a double differencing approach. In case of large height differences in the network the interval radii of the height components dominate the effective uncertainty budget. This reflects mainly the uncertainty due to tropospherical effects. It is not mitigated by double differencing. Second, it is shown that the size of the coordinates interval radii depend on the "datum definition", i.e. the strategy to solve the ill-conditioned normal equation in small GPS networks when using double differences. An optimal strategy can be defined as minimizing the maximum interval radius.

1. Introduction

Systematic effects are still a major error source in high precision GPS monitoring applications since they lead to apparent object deformations that are often difficult to separate from the real ones. Up to now, many authors analysed systematic effects mainly for GPS baselines, like e.g., [2]. Especially in the context of network RTK a multitude of correction strategies were developed; see, e.g., [6] for an overview.

It is well known that not all systematic effects can be removed during the data pre-processing or by additional parameterization. The remaining uncertainty is an additional component of the uncertainty budget. In Geodesy, [5] introduced the notion imprecision for this type of uncertainty and proposed to model it by means of deterministic error bands which are described by real intervals. They enclose the amount of uncertainty about the remaining systematics by an upper and a lower bound. The midpoints of the bands are often associated with the observed values. The corresponding mathematical theories to describe this type of uncertainty are interval mathematics or fuzzy theory.

In this paper two special topics are analyzed which are concerned with the error band approach: (i) the impact of large height differences in small GPS monitoring networks, (ii) the impact of the regularisation method needed for the inversion of the normal equations matrix, when double differencing (DD) is applied. The results are exclusively considered in the coordinate domain.

2. Mathematical concepts

In this section we briefly review the mathematical concepts of the error band approach which is based on interval mathematics. Further details on interval mathematics can be found in the textbooks of [1] or [4]. Applications to the GPS analysis were developed in [10-13].

Assuming resolved ambiguities, the interval-extension of the least-squares estimator allows to propagate interval-described observation imprecision to the estimated parameters such as the coordinates of the network points

$$[d\hat{\mathbf{x}}] = \left(\left(\mathbf{A}^\mathrm{T}\mathbf{P}\mathbf{A} \right)^- \mathbf{A}^\mathrm{T}\mathbf{P} \right)[\mathbf{y}], \tag{1}$$

where

$\quad$ $[\mathbf{y}]$ $\qquad$ is the $n \times 1$ interval-vector of observed-minus-computed values of GPS phase DD reflecting the observation imprecision,

$\quad$ $\mathbf{P}$ $\qquad$ the regular weight matrix of DD,

$\quad$ $[d\hat{\mathbf{x}}]$ $\qquad$ the resulting $u \times 1$ interval-vector of the estimated parameters.

For small GPS networks, the ($n \times u$) configuration matrix $\mathbf{A}$ has an approximate rank deficiency of three as the origin of the network is ill-determined after DD. Therefore the normal equations matrix ($\mathbf{A}^\mathrm{T}\mathbf{P}\mathbf{A}$) has to be stabilised before inversion using some sufficient additional constraints. This can be represented using a generalized inverse $\left(\mathbf{A}^\mathrm{T}\mathbf{P}\mathbf{A} \right)^-$.

As an alternative to the notation given in Eq. (1), the interval vector of parameters can be represented by its midpoint and radius $[d\hat{\mathbf{x}}] = [d\hat{\mathbf{x}}_\mathbf{m} - d\hat{\mathbf{x}}_\mathbf{r}, d\hat{\mathbf{x}}_\mathbf{m} + d\hat{\mathbf{x}}_\mathbf{r}]$, with

$$d\hat{\mathbf{x}}_\mathbf{m} = \left(\mathbf{A}^\mathrm{T}\mathbf{P}\mathbf{A} \right)^- \mathbf{A}^\mathrm{T}\mathbf{P}\,\mathbf{y}_\mathbf{m}, \tag{2a}$$

$$d\hat{\mathbf{x}}_\mathbf{r} = \left| \left(\mathbf{A}^\mathbf{T} \mathbf{P} \mathbf{A} \right)^- \mathbf{A}^\mathbf{T} \mathbf{P} \right| \mathbf{y}_\mathbf{r}, \tag{2b}$$

where $\left| \cdot \right|$ denotes the element-by-element absolute value of the matrix product. If symmetric observation intervals $\left[\mathbf{y} \right] = \left[\mathbf{y}_\mathbf{m} - \mathbf{y}_\mathbf{r}, \mathbf{y}_\mathbf{m} + \mathbf{y}_\mathbf{r} \right]$ are assumed and if the actual vector of observations is identified with $\mathbf{y}_\mathbf{m}$, the midpoint formula (2a) equals the classical least-squares estimator. The vector of interval radii (2b) describes the radius of the error bands for the estimated coordinates.

Due to the sub-distributivity property of interval vectors

$$\left(\mathbf{F}\, \mathbf{G} \right) \left[\mathbf{w} \right] \subseteq \mathbf{F} \left(\mathbf{G} \left[\mathbf{w} \right] \right), \tag{3}$$

Eq.(1) overestimates the factual range of the propagated observation imprecision which is exactly given by the zonotope Z, cf. [9]:

$$Z = \left\{ d\hat{\mathbf{x}} \in \mathbb{R}^u \,\middle|\, d\hat{\mathbf{x}} = \left(\mathbf{A}^\mathbf{T} \mathbf{P} \mathbf{A} \right)^- \mathbf{A}^\mathbf{T} \mathbf{P} \mathbf{y}, \mathbf{y} \in \left[\mathbf{y} \right] \right\}. \tag{4}$$

Considering the mathematical formulation of the pre-processing steps in a linearized form, the observation interval radii can be reformulated in terms of the imprecision (interval radii) $\mathbf{s}_\mathbf{r}$ of some basic influence parameters. That means that $\mathbf{s}_\mathbf{r}$ quantifies of the uncertainty about (or representativity of) the used values for, e.g., the temperature or the vertical total electron content (VTEC), cf. [13] for a detailed discussion

$$\mathbf{y}_\mathbf{r} = \left| \mathbf{M}\, \mathbf{F} \right| \mathbf{s}_\mathbf{r}, \tag{5}$$

where the matrix $\mathbf{M}$ stands for the mathematical operations (like double-differencing). The matrix $\mathbf{F}$ reflects the linearized functional relationship between the observation and the influence parameters.

The zonotope according to Eq. (4) can be reformulated as

$$Z = \left\{ d\hat{\mathbf{x}} \in \mathbb{R} \,\middle|\, d\hat{\mathbf{x}} = \mathbf{K}\,\mathbf{\upsilon}, \quad \mathbf{\upsilon} \in \left[-\mathbf{1}, \mathbf{1} \right] \right\}, \text{ with} \tag{6}$$

$$\mathbf{K} = \left(\mathbf{A}^\mathbf{T} \mathbf{P} \mathbf{A} \right)^- \mathbf{A}^\mathbf{T} \mathbf{P}\, \mathbf{M}\, \mathbf{F}\, diag \left(\mathbf{s}_\mathbf{r} \right), \tag{7}$$

and $\mathbf{1} = \left(1, \cdots, 1 \right)^\mathbf{T}$ the $n_{infl} \times 1$ vector of ones. The number of considered influence parameters is denoted by n_{infl}. The matrix $\mathbf{K}$ can be used to explain the transfer of the imprecision of basic influence parameters to the estimated parameters. With $\mathbf{K}$, the vector of interval radii reads $d\hat{\mathbf{x}}_\mathbf{r} = \left| \mathbf{K} \right|_1$, where $\left| \cdot \right|_1$ is the row norm of matrices.

3. Impact of height differences

3.1. Basic scenario: equal station heights

In the following we will analyse different aspects of the transfers of imprecision in small GPS networks. These studies are based on simulations assuming typical and exemplary imprecision $\mathbf{s}_\mathbf{r}$ for the basic influence parameters, cf. [13]. Three types of influence parameters can be distinguished: (i) the constants used in the apriori correction models, (ii)

the parameters used in the apriori correction models, and (iii) auxiliary information like satellite orbits or antenna phase center offsets (PCO).

If there isn't any explicit quality information about influence parameters of type (i), an error band radius s_r of 0.5 of the last significant digit can be used. For type (ii) parameters, we used in this simulation studies rather small error band of ±1.5 °C (temperature), ±1.5 mbar (pressure) and ±1.5 mbar (partial water vapour pressure), respectively, as well as $10^{15} \frac{el}{m^2}$ for the VTEC.

For the simulation, a 24-h constellation (DAY 303 2005) is used in order to assure a most homogeneous satellite sky coverage. The ambiguities were assumed to be resolved in a previous step. DD were computed for L1 phase observation. Different baselines were considered with lengths varying from 1 km to 5 km and orientations from 0° to 180° in azimuth. The height difference between the endpoints was set to 0 m. The coordinates of one endpoint were held fixed in [47°, 12°, 100 m].
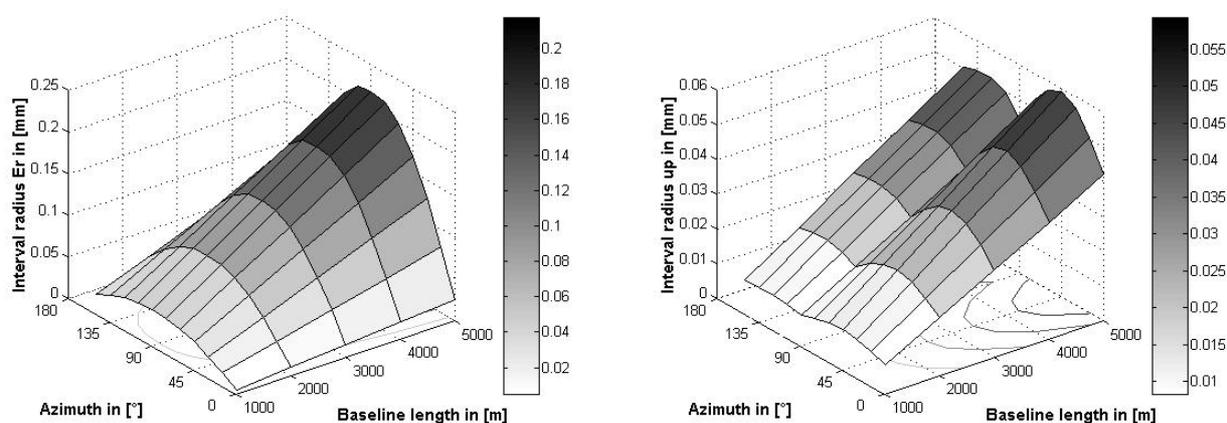

Figure 1: Interval radii for the east component (left) and height component (right) in mm

Figure 1 shows the resulting interval radii for the east and height component; please note the different scalings on the z-axes. Two main characteristics can be noted:

(1) Since most of the considered systematic effects are distance dependent ([2]), a maximum increase of the coordinate imprecision (i.e. the interval radii) with the baseline length of 0.05 ppm was found. Consequently the interval radii in East and North are larger than the interval radius in Height. Maximum values in this simulation are $N_{r,max} = 0.25$ mm, $E_{r, max} = 0.21$ mm, and $H_{r, max} = 0.06$ mm.

(2) Regarding the east and north component when varying the baseline orientation, it can be seen that the maximum amplitudes are shifted by 90°, i.e. that the interval radii are maximum in baseline direction.

Note that for short baselines the stochastic uncertainty measures (like, e.g., the formal point confidence ellipsoids) do not vary with the baseline orientation; they only slightly increase with the baseline length. See [8] for a detailed discussion on the shape and the orientation of these ellipsoids. Here the formal standard deviations are: $\sigma_N = 0.28\,\text{mm}$, $\sigma_E = 0.20\,\text{mm}$, and $\sigma_H = 0.50\,\text{mm}$.

The contribution of the different remaining systematic effects to the coordinate interval radii can be quantified and visualized based on the column vectors of **K**. Each column vector is

associated with one basic influence parameter. The vector indicates the spatial direction in the coordinate domain in which the corresponding influence parameter contributes to the coordinate imprecision. The norm of the vector quantifies the magnitude of this contribution.
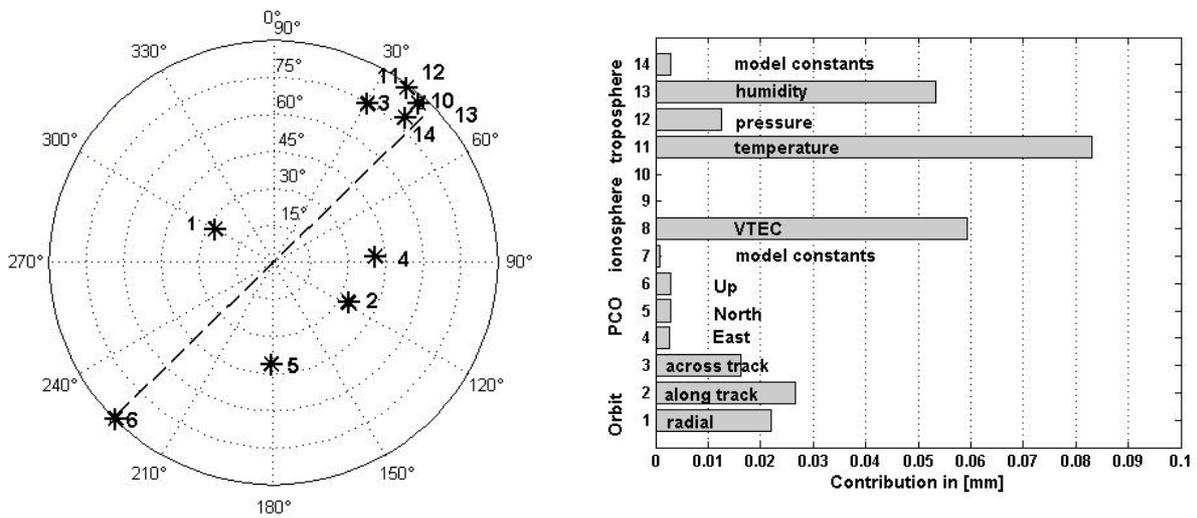

Figure 2: Contribution of basic influence parameters to the coordinate imprecision:
Left: Azimuth-elevation diagram of the directions of contribution (dashed line: baseline),
Right: Magnitude of the contributions in mm

Figure 2 shows the contribution of the basic influence parameters to the coordinate imprecision exemplarily for a 5 km baseline oriented in an azimuth direction of 45°. Most of the influence parameters contribute in direction of the baseline (dotted line). For the values used in this simulation study, the ionospheric (7-10) and tropospheric effects (11-14) contribute maximum. The uncertainty about the radial (1) and the along track (2) as well as the phase center offsets in North and East (4, 5) act perpendicular to the baseline.

The column vectors of the matrix **K** are the set of generators (edge vectors) of the zonotope Z that quantifies the point imprecision. Figure 3 shows the zonotope and the enclosing interval box exemplarily for a 5 km baseline oriented in an azimuth direction of 45°.
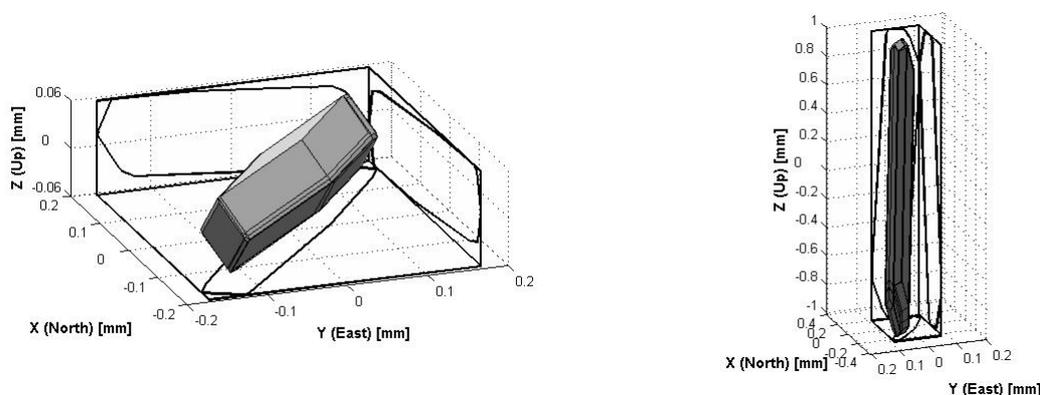

Figure 3: Zonotopes describing the factual range of coordinate imprecision for the endpoint
of a 5 km baseline oriented in azimuth 45°.
Left: no height differences between the endpoints (according to Section 3.1)
Right: height difference of 100 m between the endpoints (according to Section 3.2).

3.2. Impact of the height difference

Now the impact of large height differences between the baseline endpoints is analysed. This change in the baseline geometry mainly affects the elements in the matrix **F** as the values of the a priori correction models are now needed at different station heights (like e.g., the Saastamoinen model ([7]) for the tropospheric delay). Consequently the capability of DD to mitigate the common parts of systematic effects is weakened. Therefore, we expect that more systematic effects remain in the DD what should be correctly reflected by an increase of the coordinates' interval radii and the size of the zonotopes.

ΔH [m]	N_r [mm]	E_r [mm]	H_r [mm]
0	0.19	0.17	0.05
100	0.21	0.16	1.01
200	0.22	0.16	1.95
500	0.26	0.15	4.64
1000	0.33	0.13	8.75

Table 1: Variation of the coordinate interval radii with height differences

Table 1 gives an overview of the dependence of the interval-radii for a 5-km baseline oriented in an azimuth of 45° on the height difference between the baseline endpoints (first column) which is increased up to 1000 m. Mainly the estimated height component is affected, yielding a large increase of $8\frac{mm}{km}$ of the corresponding interval radii. Note that the size of the error ellipsoids does not change since the network geometry remains rather stable. Hence, the formal standard deviations for all stations are the same as in Section 3.1: $\sigma_N = 0.28\,\text{mm}$, $\sigma_E = 0.20\,\text{mm}$, and $\sigma_H = 0.50\,\text{mm}$.
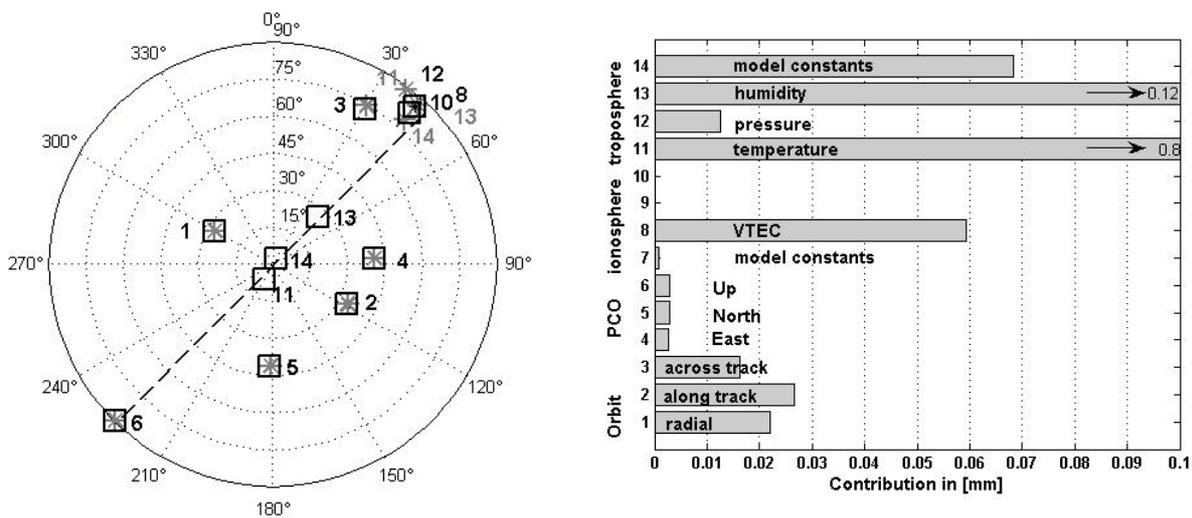

Figure 4: Contribution of basic influence parameters to the coordinate imprecision
Left: Azimuth-elevation diagram of the directions of contribution(dashed line: baseline, light grey asterisks: zero height differences, black squares: height difference of 100 m)
Right: Magnitude of the contributions in mm

Due to the particular height difference between the baseline endpoints the directions and the magnitudes of the contributions of the influence parameters change. Figure 4 shows the directions and magnitudes exemplarily for a 5 km baseline oriented in an azimuth direction of

45° and a height difference of 100 m between the baseline endpoints. The light grey asterisks indicate the directions for a zero height difference, the black squares the ones for a height difference of 100 m. The contributions of the troposphere (11, 13, 14) are now in direction of the zenith, affecting mainly the height component. Note that the magnitude and direction of the contribution of the pressure (12) do not change. This is due to the fact that the corresponding partial derivative of the Saastamoinen model is quasi independent of the height. Finally it is obvious that even for small height differences the uncertainty about the tropospheric effects dominates the coordinate imprecision, namely the one of the temperature (11). The directions and magnitudes of the other considered groups influence parameters (orbit, PCO, ionosphere) do not change.

4. Impact of the stabilisation strategy

4.1. Motivation

Now the impact of the regularisation or stabilisation strategy for solving the normal equations system for small GPS networks is studied when using DD. In the previous sections, we used a straightforward and common strategy: the coordinates of the reference station were held fixed. Alternatively, more general constraints can be applied to the coordinates to be estimated like in the "free-network" approach. This is especially of interest if the VCM of all coordinates is required in further analysis steps like, e.g., for a deformation analysis.

The normal equation can be stabilised in several ways such as:

(1) $d\hat{\mathbf{x}}_{ref} = \mathbf{0}$ (fixing the coordinates of the reference station),

(2) $d\hat{\mathbf{x}}_{ref} = \mathbf{0}, \mathbf{\Sigma}_C$ (constraining the coordinates of the reference station with, e.g., $\mathbf{\Sigma}_C = \alpha^2 \mathbf{I}$; here α was kept smaller than 3 mm in order to obtain condition numbers $cond\left(\mathbf{A}^T\mathbf{PA} + \mathbf{\Sigma}_C\right) < 10^3$),

(3) $\mathbf{G}d\hat{\mathbf{x}} = \mathbf{0}$ (no-net translation condition for all stations or for a subset of stable stations with $\mathbf{G}$ representing the nullspace of $\mathbf{A}$).

The application of one of these strategies artificially creates point positions without systematic effects (1, 3) or with neglectable systematic effects (2). In the cases (1) and (2) this is the position of the reference station; in case (3) the barycentre of the points in the constraints is free of systematic effects. Consequently the coordinate bias patterns [3] and the shape and orientation of the zonotopes change depending on the strategy used for the stabilisation of the normal equation.

4.2. Baseline scenario

Let us consider the simple but very specific case of a single baseline. Table 2 shows the variation of the interval radii and formal standard deviation of the coordinates of both baseline endpoints. We consider exemplarily a 5 km baseline oriented in an azimuth direction of 45°.

If strategy (1) is applied, the total amount of imprecision is associated to the second endpoint. The very tight constraints which are necessary for the stabilisation (here $\alpha = 2$ mm) yield very similar numerical results. Due to the symmetry of the baseline about its barycentre, strategy (3) uniformly redistributes the total amount of imprecision to both endpoints. Note that even

if strategy (3) leads to minimum standard deviation, it is not identical with the free-network approach and its minimum variance property, since the design matrix has no datum defect.

Hence, for small baselines (< 5 km) the three strategies do not change the total amount of imprecision numerically while the formal standard deviations are changed for strategy (2).

strategy	point	N_r [mm]	E_r [mm]	H_r [mm]	σ_N [mm]	σ_E [mm]	σ_H [mm]
(1)	A	0.00	0.00	0.00	0.00	0.00	0.00
	B	0.19	0.17	0.06	0.27	0.20	0.49
(2)	A	0.00	0.00	0.00	1.00	1.00	1.00
	B	0.19	0.17	0.06	1.04	1.02	1.11
(3)	A	0.09	0.08	0.03	0.14	0.10	0.25
	B	0.09	0.08	0.03	0.14	0.10	0.25

Table 2: Variations of the uncertainty measures with respect to the stabilisation strategy.

4.3. Network scenario

For networks the situation is more complex than for the case of a simple baseline. However, the mechanisms described in section 4.1 are still valid. In order to show the impact of the different stabilisation strategies a synthetic network with large height differences is generated. The reference station P0 has a height of 500 m. The baseline lengths and height differences to the other network stations are given in Table 3.

baseline	length	height difference	baseline	length	height difference
P0 - P1	1077.0	-400	P0 – P7	3026.5	400
P0 –P2	1187.4	-400	P0 –P8	3067.5	400
P0 – P3	1469.6	-400	P0 – P9	3187.4	400
P0 –P4	1999.9	0	P0 –P10	4079.2	800
P0 –P5	2061.5	0	P0 –P11	4109.7	800
P0- P6	2236.0	0	P0- P12	4199.9	800

Table 3: Baseline lengths and height differences in meters

Figure 5 shows the zonotopes and enclosing interval boxes for four different strategies. If the coordinates of the reference station are fixed (Figure 5a), this station is artificially free of systematic effects and imprecision. Consequently the systematic effects and the imprecision of this station are repartitioned to the other stations. Both increase with the height differences with respect to the reference station yielding a height depending pattern for the point imprecision, cf. Figure(5a). Since the values of the correction models do not vary linearly with the height, different amounts of imprecision of stations in the same height difference above (stations P7-P12) or beneath (stations P1-P3) the reference station are obtained.

Using strategy 3, the barycentre of the network is artificially free of imprecision. Subsequently the imprecision increases with the distance to the barycentre cf. Figure 5b. If more than one station is used in the constraints (2) the resulting zonotopes are given in Figure 5c. Figure 5d shows the results when using only P0 and P12 as a subset of stable points in condition (3).
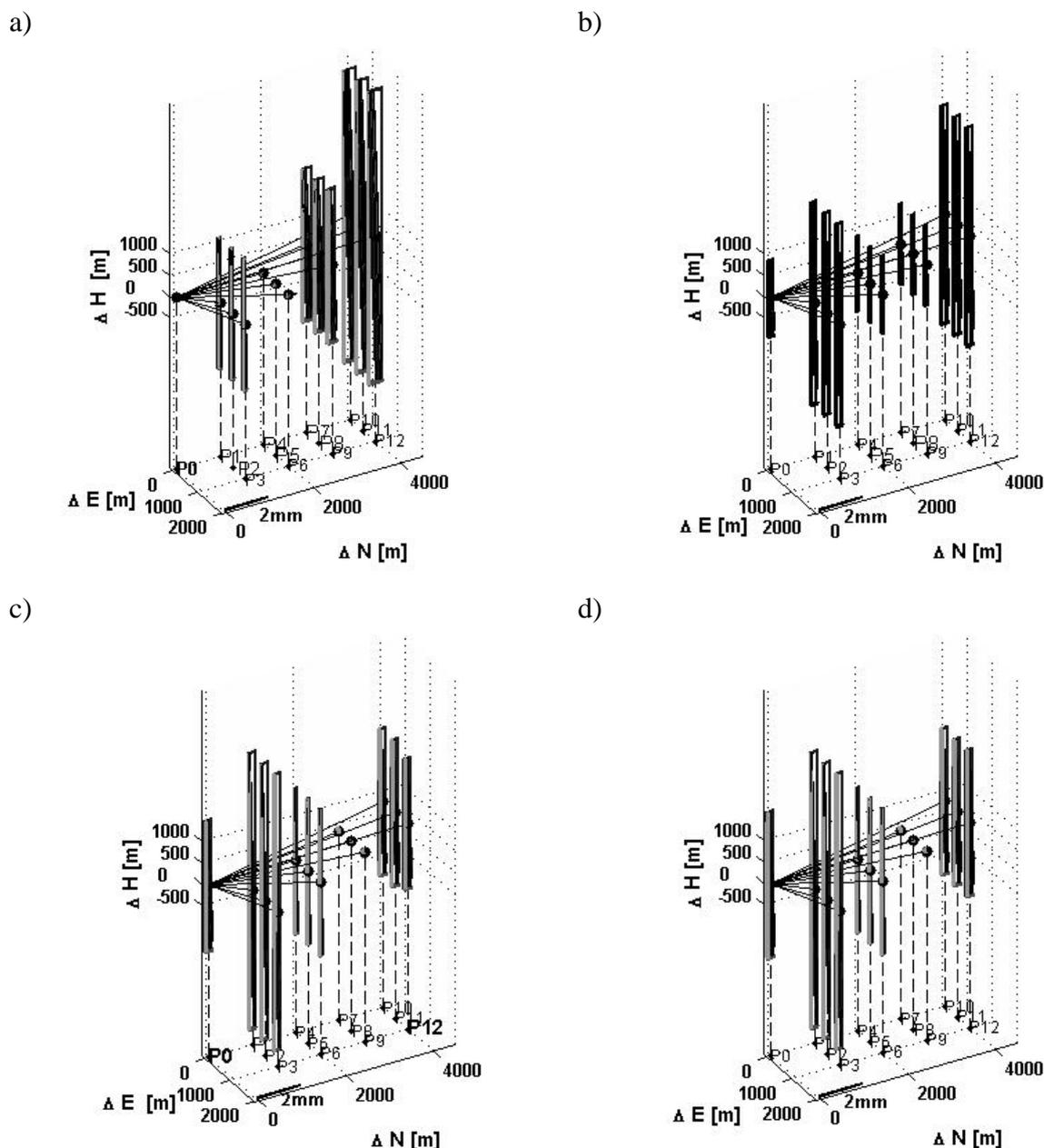
a)

b)

c)

d)

Figure 5: Variation of the size and the shape of the zonotopes applying different strategies to stabilise the normal equation

These examples underline that coordinate imprecision as well as systematic effects in the coordinate domain depend on the "datum definition". In other words, the patterns of the coordinate imprecision change with the strategy used to stabilise the ill-conditioned normal equations system when using DD. The individual repartitioning of imprecision is related to the distance of each network point to the position that is artificially free of imprecision.

5. Conclusions

In this paper the uncertainty about remaining systematic effects (imprecision) is considered as a second uncertainty component besides the random variability of the observations (stochasticity). Imprecision is described by error bands that are treated by interval methods.

It was shown that in case of large height differences in small GPS control networks the uncertainty budget is dominated by the imprecision of the height component while for horizontal networks the maximum imprecision occurs in the baseline direction.

The strategy used to stabilise the ill-conditioned normal equation changes the patterns and size of the point imprecision measures (zonotopes). All strategies introduce virtual point positions that are artificially free of systematic effects and consequently free of imprecision. The repartitioning of imprecision depends on the distance of each network point to the virtual point that is free of imprecision. These mechanisms should be incorporated in correction models for systematic effects in the coordinate domain.

Further studies will investigate optimal stabilisation strategies, e.g. by minimizing the maximum interval radii. Such strategies will lead to a homogeneous repartitioning of the point imprecision.

References:

[1] Alefeld, G. and J. Herzberger: Introduction to Interval Computations, Academic Press, New York, 1983.

[2] Beutler, G., I. Bauersima, W. Gurtner, M. Rothacher, T Schildknecht, and A. Geiger: Atmospheric refraction and other important biases in GPS carrier phase observations. In: Brunner FK (ed.) Atmospheric effects on geodetic space measurements. Monograph12, School of surveying NSW, Sydney, pp 15-44, 1988.

[3] Brunner, F.K.: On the deformation of GPS networks, Proc XX FIG Congress, Melbourne, March, pp T501.4 1- T501.4 8, 1994.

[4] Jaulin, L., M. Kieffer, O. Didrit, and E. Walter: Applied Interval Analysis, Springer, London, 2001.

[5] Kutterer, H.: Uncertainty assessment in geodetic data analysis, In: Carosio, A. and H. Kutterer (Eds.) First Int. Symp. On Robust Statistics and Fuzzy Techniques in Geodesy and GIS. Institut für Geodäsie und Photogrammetrie Bericht 295, ETH Zurich, pp 7-12, 2001.

[6] Lachapelle, G. and P. Alves: Multiple Reference Station Approach: Overview and Current Research. Journal of Global Positioning Systems 1(2): 13-136, 2002.

[7] Saastamoinen, J.: Contribution to the theory of atmospheric refraction. Part II refraction corrections in satellite geodesy. Bulletin Géodésique 107:13-34, 1973.

[8] Santerre, R.: Impact of GPS satellite sky distribution. manuscripta geodaetica 16:28-53, 1991.

[9] Schön, S.: Analyse und Optimierung geodätischer Messanordnungen unter besonderer Berücksichtigung des Intervallansatzes. Dissertation, Deutsche Geodätische Kommission C 567. München, 2003.

[10] Schön, S. and H. Kutterer: Imprecision in Geodetic Observations – Case Study GPS Monitoring Network. In: Stiros, S. and S. Pytharouli (Eds.) Proc 11th: FIG Int. Symp. on Deformation Measurements. Geodesy and Geodetic Applications Lab., Patras University. Publication No.2: 471-478, 2003.

[11] Schön, S. and H. Kutterer: Realistic uncertainty measures for GPS observations. In: Sanso, F. (Ed.): A Window on the Future of Geodesy. Springer Berlin, pp 54-59, 2005.

[12] Schön, S. and H. Kutterer: Using Zonotopes for Overestimation-Free Interval Least-Squares - Some Geodetic Applications. Reliable Computing, 11(2):137-155, 2005.

[13] Schön, S. and H. Kutterer: Uncertainty in GPS networks due to remaining systematic errors – the interval approach. Journal of Geodesy (in press).